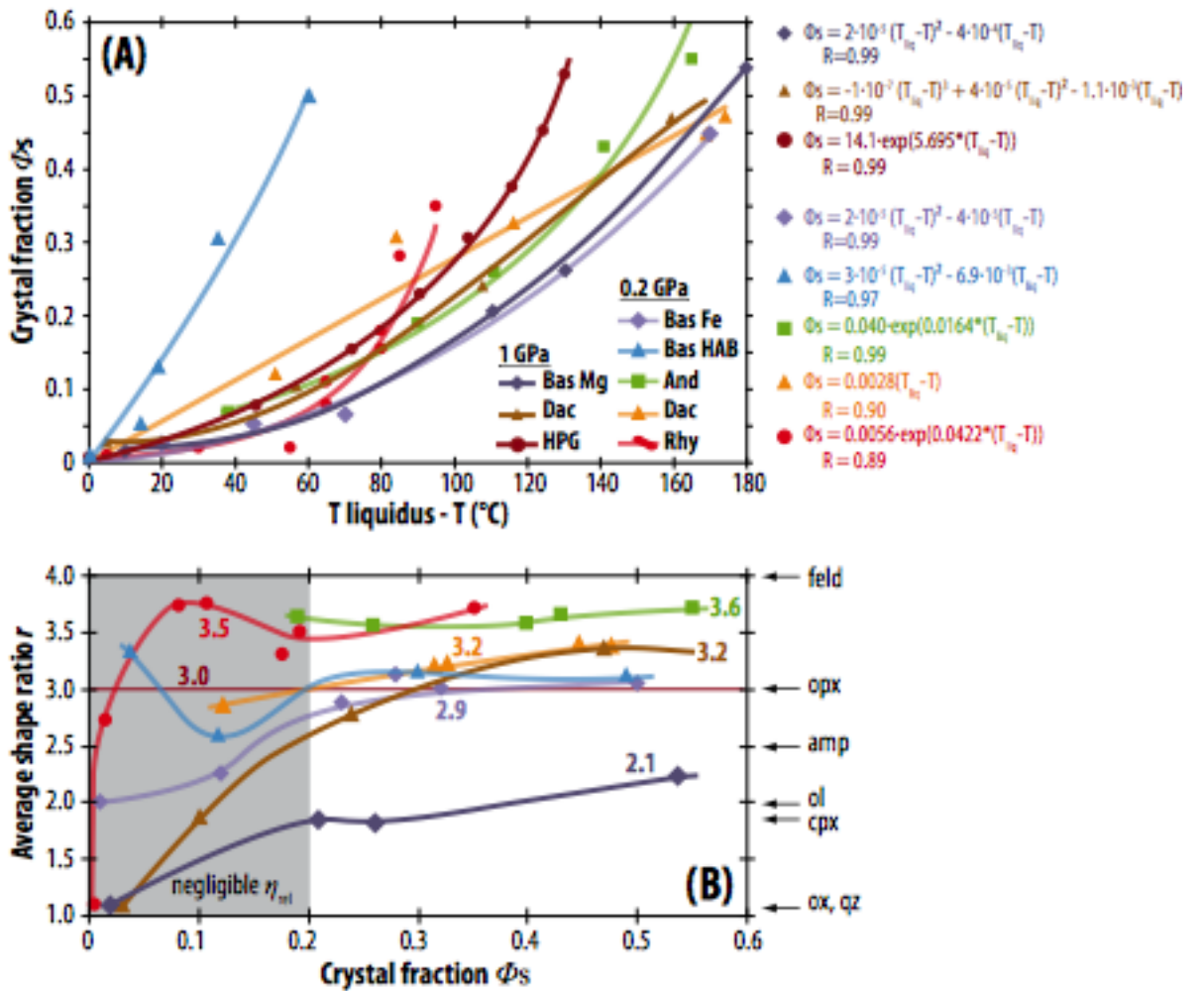
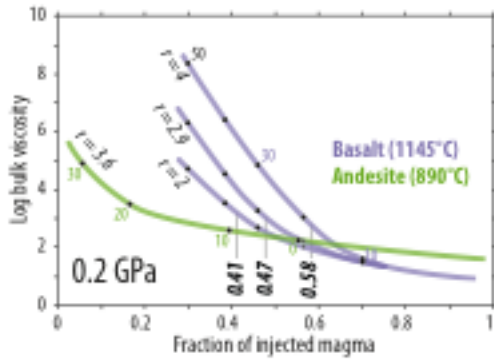


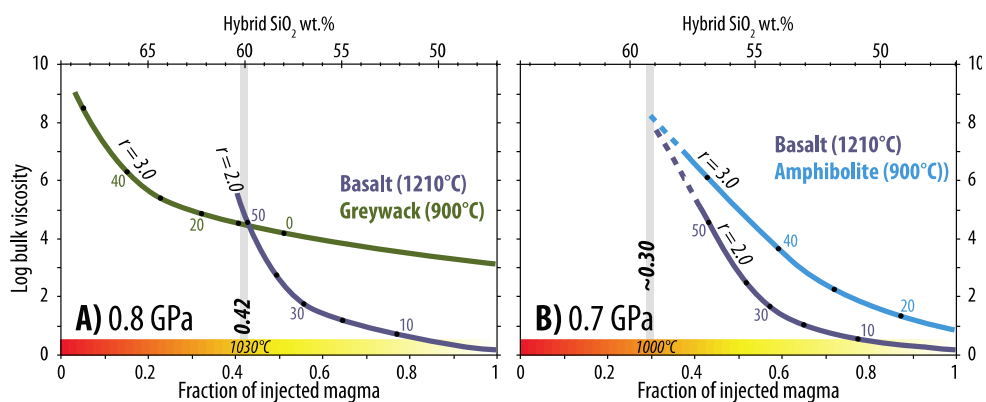
Supplementary Figure 1 | Experimental sample set up. Sketches of samples used for mixing experiments consisting in the vertical juxtaposition of 2 and 4 layers simulating simple shear deformation by twisting, and allowing strain partitioning between end-members. SEM images presented in Fig. 1 (main text) are tangential sections of different experiments.



Supplementary Figure 2 | Crystal fraction and magma viscosity. (a) Evolution of the crystal fraction Φ_s with temperature for each magma composition used in the calculations, expressed as the difference relative to the liquidus temperature. (b) Average shape ratio of the crystal suspension in the different magmas used for viscosity calculations. The grey shaded area below $\Phi_s = 0.2$ highlights the domain where crystal fraction has little effect on the relative viscosity. At $\Phi_s > 0.2$, most of the magmas have an average crystal shape ratio between 3.0 and 3.6, except the feldspar-poor basalt from Saint Vincent (Bas Mg). Numbers next to each curve indicate the average shape ratio used to calculate the viscosity of each magma.



Supplementary Figure 3 | Effect of the shape ratio of crystals on mixing. The shape ratio influences the relative viscosity and consequently the bulk viscosity, hence mixing. While the average shape ratio varies little over the crystal fraction 0.2 – 0.6, small differences in composition of otherwise similar magmas may affect their average crystal shape ratio, and consequently their respective bulk viscosity (compare Bas Fe and Bas Mg on Fig. 4 in main text). The basalt from Skaergaard intrusion¹ is mostly composed of clinopyroxene, plagioclase and magnetite, and has an intermediate average shape ratio. As shown, a lower shape ratio (such as with an assemblage dominated by olivine) decreases the amount of injected mafic magma fraction required to reach favourable conditions for magma mixing, with a mixing ratio of 0.47. In contrast, if the crystallising phase assemblage is dominated by plagioclase (larger shape ratio) a larger fraction of a mafic magma (0.58) is necessary to produce a hybrid magma.



Supplementary Figure 4 | Effect of host rock temperature on mixing in the lower crust. The results are shown for hybridization of (a) basalt - greywacke and, (b) basalt - amphibolite. The hatched vertical fields correspond to mixing conditions when the crust is at 750°C (shown on Fig 5). Note that for the amphibolite case, equal viscosities are reached at crystal contents beyond 50%, ie outside the calibrated range of the viscosity equation used here, and mixing is unlikely in this case.

Supplementary Table 1 | Compositions of the starting materials

Oxide	Htn	Dacite	Basalt*
SiO ₂	68.8	2	65.58 25
TiO ₂	0.01	1	0.81 7
Al ₂ O ₃	19.8	2	15.93 14
FeO _{total}	0.00	0	5.21 25
MnO	0.00	0	1.37 5
MgO	0.00		0.16
CaO	3.37	8	3.99 9
Na ₂ O	8.06	28	4.94 14
K ₂ O	0.01	2	1.98 9
P ₂ O ₅	-	-	0.49
Total	100.00	100.00	100.00

Haplotonalite (Htn) and dacite glass analyses were performed by EMPA, with standard deviation indicated by italic font.

* XRF analysis²

Supplementary Table 2 | Experimental results on single compositions

Material	Exp. #	r (mm)	L (mm)	Total strain	Step strain	Strain rate (s ⁻¹)	T (°C)	Jacket	Jacket contrib.	Log stress (Pa)	Step viscosity	Viscosity (Pa s)	Err. max viscosity
PP300	7.46	7.21	0.4	0.09 0.02 0.06 0.15 0.10 0.01 0.07 0.11 0.08 0.15	0.09	3.9E-05	700	Cu	1%	7.8	12.08	12.08	1.1
					0.02	8.9E-05	700		1%	7.8	11.86		1.0
					0.06	4.6E-05	750		2%	7.3	11.67		1.0
					0.15	1.0E-04	750		1%	7.6	11.56	11.56	1.0
					0.10	2.1E-04	750		1%	7.8	11.46		0.9
					0.01	1.3E-04	800		24%	6.3	10.20	10.20	0.7
					0.07	7.0E-05	900		12%	4.6	8.76		0.5
					0.11	2.0E-04	900		14%	4.8	8.45	8.37	0.4
					0.08	3.5E-04	900		15%	4.9	8.31		0.4
					0.15	1.3E-03	900		18%	5.1	7.98		0.4
Htn	7.49	10.31	0.9	0.02 0.06 0.06 0.08 0.09 0.12 0.07 0.12 0.06 0.16	0.02	5.1E-05	900	Fe	13%	4.3	8.62		0.5
					0.06	2.1E-04	900		15%	4.5	8.14	8.17	0.4
					0.06	4.3E-04	900		17%	4.7	8.05		0.4
					0.08	1.3E-03	900		20%	5.0	7.85		0.4
					0.09	9.8E-05	1000		33%	3.2	7.17	7.07	0.5
					0.12	2.4E-04	1000		30%	3.4	6.98		0.5
					0.07	7.1E-05	1100		30%	-	<5		
					0.12	4.4E-05	750		28%	5.6	9.62		0.7
					0.06	8.9E-05	750		26%	5.6	9.99	9.79	0.7
					0.16	1.7E-04	750		20%	6.0	9.75		0.7
Dacite	PP301	7.48	8.80	0.8	0.01 0.08 0.19 0.02 0.06 0.07	0.01	8.2E-05	Cu	36%	5.2	9.32		0.6
					0.08	9.2E-05	800		27%	5.6	9.63	9.42	0.7
					0.19	1.8E-04	800		29%	5.5	9.30		0.6
					0.02	8.4E-05	850		44%	4.8	8.88		0.6
					0.06	3.4E-04	850		45%	4.7	8.21	8.49	0.4
					0.07	7.2E-04	850		36%	5.2	8.39		0.5
					0.19	8.0E-05	1100		19%	5.7	9.83	9.70	0.6
					0.13	1.6E-04	1100		19%	5.8	9.57		0.6
					0.08	8.5E-05	1120	Fe	26%	4.5	8.56	8.65	0.5
					0.04	3.8E-04	1120		28%	5.3	8.74		0.5
Basalt	PP247	7.48	10.30	0.4	0.06 0.06 0.06 0.09	0.06	4.4E-05	Cu	40%	2.0	6.38	6.14	0.6
						0.06	5.1E-05		42%	1.6	5.89		0.7
						0.02	3.1E-05		-	-	<5		-
						0.06	1.4E-04		-	-	<5		-
						0.09	3.1E-04		-	-	<5		-
PP153	7.47	7.14	0.3	0.09	0.06	4.4E-05	1140	Fe	-	-	<5	-	-
					0.06	5.1E-05	1140		-	-	<5	-	-
					0.09	3.1E-04	1170		-	-	<5	-	-

Exp. # refers to the number of experiment, r and L are the sample radius and length (in mm), respectively. Some experiments were conducted through different steps, with varied temperature or strain rates.

Supplementary Table 3 | Experimental results on mixing between dry haplotonalite and dacite compositions

Material	Exp. #	r (mm)	L (mm)	Total strain	Step strain	Strain rate (s ⁻¹)	T (°C)	Jacket	Jacket contrib.	Log stress (Pa)	Step viscosity	Viscosity (Pa s)	Err. max viscosity
Htn + Dacite	PP302	7.40	8.17	4.3	0.04	5.9E-05	850	Fe	32%	5.0	9.23	9.11	0.6
					0.06	1.3E-04	850		27%	5.3	9.15		0.6
					2.77	3.3E-04	850		25%	5.5	9.01	8.23	0.5
					1.41	6.4E-04	850		22%	5.9	9.05		0.5
	PP303	7.48	8.20	8.3	0.05	3.5E-05	900	Fe	32%	4.1	8.59	8.82	0.5
					0.15	1.0E-04	900		28%	4.4	8.36		0.5
					0.95	3.3E-04	900		24%	4.6	8.04		0.4
					3.46	5.4E-04	900	Fe	25%	4.7	7.94		0.4
					0.11	3.3E-04	850		33%	5.3	8.80	8.23	0.5
					3.53	5.4E-04	850		26%	5.6	8.84		0.5
	PP349	7.47	6.46	1.7	1.70	2.1E-04	950	iron	-	-	-	7.6	-
	PP346	7.49	4.78	1.7	1.68	4.2E-04	1000	iron	-	-	-	7.1	-

Exp. # refers to the number of experiment, r and L are the sample radius and length (in mm), respectively. Some experiments were conducted through different steps, with varied temperature or strain rates. Numbers italicized are calculated values.

Supplementary Table 4 | Experimental results on mixing between dry haplotonalite and basalt compositions

Material	Exp. #	r (mm)	L (mm)	Total strain	Step strain	Strain rate (s ⁻¹)	T (°C)	Jacket	Jacket contrib.	Log stress (Pa)	Step viscosity	Viscosity (Pa s)	Err. max viscosity
dry Htn+Basalt	PP149	7.47	10.48	1.9	1.93	8.9E-05	900	Fe	11%	4.7	8.76	8.76	0.5
	PP235	7.47	8.73	0.5	0.50	2.9E-03	1050	Fe	40%	3.7	6.32	6.32	0.5
	PP155	7.25	8.65	1.3	1.26	2.3E-04	1150	Fe	-	-	-	4.6	-
	PP156	6.91	8.64	4.9	4.92	3.1E-04	1160	Fe+steel	-	-	-	4.4	-
	PP157	6.91	8.47	3.6	3.62	4.4E-04	1170	Fe+steel	-	-	-	4.2	-
	PP160	6.91	6.31	3.1	3.10	9.3E-04	1170	Fe+steel	-	-	-	4.2	-
	PP161	6.91	5.28	3.1	3.11	4.8E-04	1170	Fe+steel	-	-	-	4.2	-
	PP164	6.91	8.27	3.9	3.93	4.7E-04	1170	Fe+steel	-	-	-	4.2	-
	PP151	7.47	9.83	1.3	0.26	7.2E-05	1200	Fe	-	-	-	-	-
					0.25	2.3E-04	1200		-	-	-	3.5	-
					0.82	6.7E-04	1200		-	-	-	-	-
	PP176	6.92	6.64	3.8	3.78	5.2E-04	1200	Fe+steel	-	-	-	3.5	-

Exp. # refers to the number of experiment, r and L are the sample radius and length (in mm), respectively. Some experiments were conducted through different steps, with varied temperature or strain rates. Numbers italicized are calculated values.

Supplementary Table 5 | Experimental results on mixing between hydrous haplotonalite and basalt compositions

Material	Exp. #	r (mm)	L (mm)	Total strain	Step strain	Strain rate (s ⁻¹)	T (°C)	Jacket	Jacket contrib.	Log stress (Pa)	Step viscosity	Viscosity (Pa s)	Err. max viscosity
Hydrous Htn+Basalt	PP265	7.48	5.33	0.7	0.20	4.3E-05	600	copper	4%	7.3	11.64	11.42	1.0
					0.21	8.5E-05	600		4%	7.3	11.32		0.9
					0.33	2.3E-04	600		4%	7.7	11.31		0.9
	PP258	7.46	10.93	1.7	0.03	4.2E-05	715	Cu	13%	6.5	10.85	10.77	0.8
					0.14	8.8E-05	715		5%	6.6	10.69		0.8
					0.85	4.8E-04	715		4%	7.5	10.84		0.8
	PP285	7.41	7.39	2.4	0.69	8.1E-04	715	Fe	4%	7.6	10.69	8.57	0.7
					0.02	4.3E-05	950		33%	4.3	8.69		0.5
					0.33	2.9E-04	950		34%	4.9	8.44		0.4
	PP295	7.35	7.37	2.0	2.03	5.9E-04	950	Fe	36%	5.0	8.22	0.4	0.4
					0.69	9.6E-05	975		31%	4.2	8.26		0.4
	PP296	6.89	8.21	5.1	1.34	2.0E-04	975	Fe+steel	32%	4.3	8.03	8.14	0.4
					0.45	1.0E-04	985		35%	3.6	7.64		0.5
					0.45	3.1E-04	985		33%	4.2	7.71		0.4
	PP261	7.46	8.31	1.3	4.18	8.0E-04	985	Fe+steel	37%	4.5	7.58	7.65	0.4
					0.12	9.0E-05	1000		48%	3.1	7.48		1.0
					0.06	4.3E-05	1000		49%	3.1	7.17		1.1
	PP293	6.90	8.71	0.7	1.08	2.8E-04	1000	Fe+steel	50%	3.3	6.85	6.18	1.0
					0.35	2.1E-04	1020		63%	2.6	6.32		1.2
					0.39	8.7E-04	1020		61%	3.0	6.04		1.2

Exp. # refers to the number of experiment, r and L are the sample radius and length (in mm), respectively. Some experiments were conducted through different steps, with varied temperature or strain rates.

Supplementary Table 6 | Source of data for the parameters of the viscosity equation

Reference	Crystal shape ratio
3	1
4	<1.5
5	1.5
6	2.4
7	3
8	4.9
9	5

Supplementary Table 7 | Symbols and parameter values used in thermal calculations

Parameter	Symbol	Value	Unit
Final temperature	T	-	°C
Fraction of mafic magma injected	x	-	-
Heat capacity of felsic and mafic magmas	C _{f-m}	1.26	J g ⁻¹ K ⁻¹
Mass fraction of crystal dissolved in felsic magma	X _f	variable	-
Heat of fusion of crystals in felsic magma	L _f	293	J g ⁻¹
Mass fraction of new crystals formed in mafic magma	X _m	variable	-
Heat of fusion of crystals in mafic magma	L _m	418	J g ⁻¹

Supplementary Table 8 | Liquidus temperatures and bulk water content for felsic and mafic end members, and input temperatures used for each end-member in the mixing calculations shown in Fig. 5-7 and Supplementary Figures 3, 4.

	Composition	Initial T (°C)	Liquidus T (°C)	Bulk H ₂ O (wt%)	Reference
0.7-1 GPa	Basalt Mg	1210	1210	6.0	10
	Dacite Pinatubo	750	1000	13.0	11
	Dacite H ₂ O undersat.	750	1000	9.0	11
	Rhyolite HPG	750	1030	13.0	12
0.2 GPa	Rhyolite HPG undersat.	750	1030	3.0	12
	Greywacke	750	1060	1.8	13
	Amphibolite	750	1060	4.0	14
	Basalt Fe	1145	1145	6.0	1
	Basalt HAB	980	980	6.0	15
	Andesite Mt Pelée	890	1040	6.1	16
	Dacite Pinatubo	776	930	7.0	17
	Rhyolite Unzen	780	850	6.0	18

Supplementary References

1. Botcharnikov, R. E., Almeev, R. R., Koepke, J., & Holtz, F. Phase relations and liquid lines of descent in hydrous ferrobasalt—implications for the Skaergaard intrusion and Columbia River flood basalts. *J. Petrol.* **49**, 1687-1727 (2008).
2. Andújar, J., Scaillet, B., Pichavant, M., & Druitt, T. H. Differentiation conditions of a basaltic magma from Santorini and its bearing on andesitic/dacitic magma production. In *AGU Fall Meeting Abstracts* (Vol. 1, p. 2354) (2010).
3. Lejeune, A. M., & Richet, P. Rheology of crystal-bearing silicate melts: An experimental study at high viscosities. *J. Geophys. Res.* **100**, 4215-4229 (1995).
4. Champallier, R., Bystricky, M., & Arbaret, L. Experimental investigation of magma rheology at 300 MPa: From pure hydrous melt to 76 vol.% of crystals. *Earth Planet. Sci. Lett.* **267**, 571-583 (2008).
5. Scott, T., & Kohlstedt, D. L. The effect of large melt fraction on the deformation behavior of peridotite. *Earth Planet. Sci. Lett.* **246**, 177-187 (2006).
6. Caricchi, L., Burlini, L., Ulmer, P., Gerya, T., Vassalli, M., & Papale, P. Non-Newtonian rheology of crystal-bearing magmas and implications for magma ascent dynamics. *Earth Planet. Sci. Lett.* **264**, 402-419 (2007).
7. Rutter, E. H., & Neumann, D. H. K. Experimental deformation of partially molten Westerly granite under fluid-absent conditions, with implications for the extraction of granitic magmas. *J. Geophys. Res.* **100**, 15697-15715 (1995).
8. Vona, A., Romano, C., Dingwell, D. B., & Giordano, D. The rheology of crystal-bearing basaltic magmas from Stromboli and Etna. *Geochim. Cosmochim. Acta*, **75**, 3214-3236 (2011).
9. Picard, D., Arbaret, L., Pichavant, M., Champallier, R., & Launeau, P. Rheology and microstructure of experimentally deformed plagioclase suspensions. *Geology* **39**, 747-750 (2011).
10. Melekhova, E., Annen, C., & Blundy, J. Compositional gaps in igneous rock suites controlled by magma system heat and water content. *Nature Geo.* **6**, 385-390 (2013).
11. Prouteau, G., & Scaillet, B. Experimental constraints on the origin of the 1991 Pinatubo dacite. *J. Petrology* **44**, 2203-2241 (2003).
12. Johannes, W., & Holtz, F. *Petrogenesis and experimental petrology of granitic rocks* (Vol. 335). Berlin: Springer (1996).
13. Montel, J. M., & Vielzeuf, D. Partial melting of metagreywackes, Part II. Compositions of minerals and melts. *Contr. Mineral. Petrol.* **128**, 176-196 (1997).
14. Sisson, T. W., Ratajeski, K., Hankins, W. B., & Glazner, A. F. Voluminous granitic magmas from common basaltic sources. *Contr. Mineral. Petrol.* **148**, 635-661 (2005).
15. Sisson, T. W., & Grove, T. L. Experimental investigations of the role of H₂O in calc-alkaline differentiation and subduction zone magmatism. *Contr. Mineral. Petrol.* **113**, 143-166 (1993).
16. Martel, C., Pichavant, M., Holtz, F., Scaillet, B., Bourdier, J. L., & Trainea, H. Effects of fO₂ and H₂O on andesite phase relations between 2 and 4 kbar. *J. Geophys. Res.* **104**, 29453-29470. (1999).
17. Scaillet, B., & Evans, B. W. The 15 June 1991 eruption of Mount Pinatubo. I. Phase equilibria and pre-eruption P-T-fO₂-fH₂O conditions of the dacite magma. *J. Petrol.* **40**, 381-411 (1999).
18. Tomiya, A., Takahashi, E., Furukawa, N., & Suzuki, T. Depth and evolution of a silicic magma chamber: Melting experiments on a low-K rhyolite from Usu volcano, Japan. *J. Petrol.* **51**, 1333-1354 (2010).